

1 **DIURNAL, SEASONAL AND SOLAR CYCLE VARIATION OF TOTAL ELECTRON**
2 **CONTENT AND COMPARISON WITH IRI-2016 MODEL AT BIRNIN-KEBBI**

3 ^{1,*}Aghogho Ogwala, ¹Emmanuel Olufemi Somoye, ³Olugbenga Ogunmodimu, ¹Rasaq
4 Adewemimo Adeniji-Adele, ¹Eugene Oghenakpobor Onori, ²Oluwole Oyedokun

5 ^{1,*} Department of Physics, Lagos State University, Lagos, Nigeria.

6 ²Department of Physics, University of Lagos, Nigeria.

7 ³ Department of Electrical Engineering, Manchester Metropolitan University, United Kingdom.

8 **ABSTRACT**

9 The ionosphere is the major error source for the signals of Global Positioning System (GPS)
10 satellites. In the analysis of GPS measurements, ionospheric error is somewhat assumed to be a
11 nuisance. The error induced by the ionosphere is proportional to the number of electrons along the
12 line of sight (LOS) from the satellite to receiver and can be determined in order to study the diurnal,
13 seasonal, solar cycle and spatial variations of the ionosphere during quiet and disturbed conditions.
14 In this study, we characterize the diurnal, seasonal and solar cycle variation of observed (OBS)
15 total electron content (TEC) and compare the result with the International Reference Ionosphere
16 (IRI-2016) model. We obtained TEC from a dual frequency GPS receiver located at Birnin-Kebbi
17 Federal Polytechnic (BKFP) in Northern Nigeria (geographic location: 12.64° N; 4.22° E; 2.68°
18 N dip) for the period 2011 – 2014. We observed differences between the diurnal variation OBS-
19 TEC and IRI-2016 model for all hours of the day except during the post-midnight hours. Slight
20 post-noon peaks in the daytime maximum and post-sunset decrease and enhancement are observed
21 in the diurnal variation of OBS-TEC during the equinoxes. On a seasonal scale, we observed that
22 OBS-TEC values were higher in the equinoxes than the solstices only in 2012. Whereas in 2011,

23 September equinox and December solstice recorded higher magnitude followed by March equinox
24 and lowest in June solstice. In 2013, December solstice magnitude was highest, followed by the
25 equinoxes and lowest in June solstice. In 2014, March equinox and December solstice magnitude
26 were higher than September equinox and June solstice magnitude. June solstice consistently
27 recorded the lowest values for all the years. OBS-TEC is found to increase from 2011 to 2014,
28 thus revealing solar cycle dependence.

29 **KEYWORDS:** TEC; diurnal; seasonal; variation; solar cycle 24; IRI-2016.

30 **CORRESPONDING AUTHOR PHONE:** +234 8055650264

31 **CORRESPONDING AUTHOR E-MAIL:** ogwala02@gmail.com

32
33
34
35
36
37
38
39
40
41
42
43
44
45
46
47
48

49 **1 INTRODUCTION**

50 Ionospheric irregularities as a result of inhomogeneity in electron density leads to variations in the
51 intensity of radio signals (Somoye, 2010; Ogwala et al. 2018, Ogunmodimu et al. 2018). Akala et
52 al., (2011) posted that the variable nature of the equatorial/ low latitude ionosphere do adversely
53 affect communication and navigation/ satellite systems in the region. The equatorial/ low latitude
54 ionosphere exhibits unique features such as the seasonal anomaly, semi-annual anomaly,
55 equinoctial anomaly, noon bite-out, spread-F, equatorial electrojet (EEJ) and equatorial plasma
56 bubbles (EPB) (Stankov, 2009; Maruyama et al., 2004; Jee et al., 2004; Codrescu et al., 1999).

57 For many decades, scientists have been studying these peculiar ionospheric features and their roles
58 in trans-ionospheric electromagnetic radio wave propagation using different techniques and
59 instruments. One of the instruments often used is the GPS receiver. The GPS receiver provide
60 direct measurements from satellites. Their sounding capacity extends to the topside of the
61 ionosphere, and is affected by time and space constraints (Ciraolo and Spalla, 2002). Recently,
62 dual frequency GPS receiver is the most efficient method used to eliminate the effect of the
63 ionosphere on radio signals. This method combine signals in different L band frequencies, L1
64 (1575 MHz) and L2 (1228 MHz) (Bolaji et al., (2012; Alizadeh et al., 2013).

65 Almost all space geodetic techniques transmit signals in at least two different frequencies
66 for better accuracy (Alizadeh et al., 2013). The signals are then combined linearly in order to
67 eliminate the effect of the ionosphere on radio signals. The ionospheric effect on radio signal is
68 proportional to the total electron content (TEC), which is defined as the number of electrons per
69 square meter from satellite in space to receiver on ground as shown in Eq. (1).

70 $TEC = \int n_e(s)ds$ (1)

71 It is measured in multiples of TEC units (1 TECU = 10^{16} el/m²). Due to the dispersive nature of
72 the ionosphere, there is a time delay between the two frequencies of a GNSS signal as it propagate
73 through the ionosphere as shown in Eq. (2) as $\Delta t = t_2 - t_1$. Thus,

$$74 \quad \Delta t = \left(\frac{40.3}{c} \right) \times \frac{TEC}{\left[\left(\frac{1}{f_2^2} \right) - \left(\frac{1}{f_1^2} \right) \right]} \quad (2)$$

75 Where c is speed of light and f is frequency. Hence, Δt measured between the L1 and L2
76 frequencies is used to evaluate TEC along the ray path.

77 When Global Navigation Satellite System (GNSS) signals propagate through the ionosphere, the
78 carrier experiences phase advance and the code experiences a group delay due to the electron
79 density along the line of sight (LOS) from the satellite to the receiver (Bagiya et al., 2009; Tariku,
80 2015). Thus, the carrier phase pseudo ranges are measured too short, and the code pseudo ranges
81 are measured too long compared to the geometric range between the satellite and the receiver. This
82 results in a range error of the positioning accuracy provided by a GPS receiver. The range error
83 due to TEC in the ionosphere varies from hundreds of meters at mid-day, during high solar activity
84 when the satellite is near the horizon of the observer, to a few meters at night during low solar
85 activity, with the satellite positioned at zenith angle (Bagiya et al., 2009). By measuring this delay
86 using dual frequency GPS receivers, properties of the ionosphere can be inferred and used to
87 monitor space weather events such as GNSS, HF communications, Space Based Observation
88 Radar and Situational Awareness Radar, etc. Ionospheric delay (proportional to TEC) is the highest
89 contributor to GPS positioning error (Alizadeh et al., 2013; Bolaji et al., (2012).

90 TEC in the ionosphere can also be studied using empirical ionospheric model such as the
91 International Reference Ionosphere (IRI). IRI is a joint undertaking by the Committee on Space
92 Research (COSPAR) and International Union of Radio Science (URSI) with the goal of developing

93 and improving an international standard for the parameters in earth's ionosphere (Bilitza et al.,
94 2014). An updated version has been recently developed to cater for lapses of previous models. IRI
95 provides the vertical TEC (VTEC) from the lower boundary (60 – 80 km) to a user-specific upper
96 boundary (Bilitza et al., 2016).

97 In the past few decades, studies on the temporal and spatial variations of TEC have gained
98 popularity in the scientific community (Wu et al., 2008). However, understanding the variability
99 of TEC will also go a long way in obtaining the positioning accuracy of GNSS under disturbed
100 and quiet conditions. As such, previous studies (e.g. Ayorinde et al., 2016; Bhuyan and Borah,
101 2007; Maruyama et al., 2004; Jee et al., 2004; Balan et al., 1994; Rama Rao et al., 2006a, b, c;
102 Rama Rao et al., 1985; Bolaji et al. 2012; Wanninger, 1993; Akala et al., 2013; Komjathy et al.,
103 1998; Langley et al., 2002 Sunda et al., 2013; Torr and Torr, 1973; Tsai et al., 2001 and references
104 therein) investigated the global distribution of TEC variations and its characteristics at all latitudes,
105 during different solar cycle phases under disturbed and quiet conditions.

106 Studies of Rama Rao et al. (2006a, b) in the Indian sector and Wanninger (1993) in the
107 Asian sector reported maximum day-to-day variability in TEC at the Equatorial Ionization
108 Anomaly (EIA) crest regions, increasing peak value of TEC with increase in integrated equatorial
109 electrojet (IEEJ) strength, maximum monthly average diurnal variations during equinox months
110 followed by winter months and lowest during summer months. They also reported positive
111 correlation of TEC and EEJ and the spatial variation of TEC in the equatorial region. Titheridge
112 (1974) and Langley et al. (2002) attributed the lowest TEC values during the summer seasons to
113 low ionization density resulting from reduced O/ N₂ ratio (production rates) as a result of increased
114 scale height. Bhuyan and Borah (2007) working in the Indian sector and Komjathy et al. (1998)
115 and Lee and Reinisch (2006) while studying in the American sector compared TEC derived from

116 GPS receivers with IRI model in the equatorial/ low latitude sector and inferred that the diurnal
117 amplitude of TEC is higher during the equinoxes followed by December solstices and lowest in
118 June solstice, i.e., observing winter anomaly in seasonal variation. They further reported
119 discrepancies between IRI model and their measured values during most hours of the day at their
120 various locations. Malik et al. (2016) on their studies over the Malaysian peninsular reported
121 higher IRI values than observed maximum useable frequency (MUF) values but behaves similarly
122 diurnally and seasonally with no clear trend. Akala et al. (2013) on the comparison of equatorial
123 GPS-TEC observations over an African station and an American station during the minimum and
124 ascending phases of solar cycle 24 reported that seasonal VTEC values were maximum and
125 minimum during March equinox and June solstice respectively, during minimum solar cycle phase
126 at both stations. They also reported that during the ascending phase of solar cycle 24, minimum
127 and maximum seasonal VTEC values were recorded during December solstice and June solstice
128 respectively. They further showed that IRI-2007 model predicted better in the American sector
129 than the African sector.

130 The aim of this paper is (i) to characterize TEC on diurnal, seasonal and solar cycle scales
131 in the Nigerian Equatorial ionosphere (ii) to compare OBS-TEC with IRI-2016 model in order to
132 find if the model underestimates or overestimates TEC values at the African longitudinal sectors.
133 In section 2, we describe the data and methodology. Section 3 shows the result and discussion
134 while concluding remarks are in section 4.

135 **2 DATA AND METHODOLOGY**

136 **2.1 DATA**

137 The Receiver Independence Exchange (RINEX) Observation GPS data files were
138 downloaded daily from NIGNET website (www.nignet.net) and processed using Bernese software

139 and GPS TEC analysis software. The RINEX file contains 60 iteration data (i.e. in 1 minute time
 140 resolution). The GPS-TEC analysis software was designed by Gopi Seemala of the Indian Institute
 141 of Geomagnetism. The summary of this application is to read raw data, processes cycle slips in
 142 phase data, reads satellite biases from the International GNSS services (IGS) code files (and
 143 calculates them if unavailable), and calculates receiver bias, inter-channel biases for different
 144 satellites in the constellation, and finally plots the VTEC values on the screen and writes the ASCII
 145 output files (*CMN) for STEC and (*STD) for VTEC in the same directory of the data files. Effect
 146 due to multipath is eliminated by using a minimum elevation angle of 50°.

147 Observation GPS-TEC obtained from the TEC analysis software is the slant TEC (STEC)
 148 and vertical TEC (VTEC). STEC is polluted with several biases that must be eliminated to get
 149 VTEC. VTEC is calculated from the daily values of STEC using Eq. (3).

$$150 \quad VTEC = (STEC - [b_R + b_S + b_{RX}])/S(E) \quad (3)$$

151 Where b_R , b_S , and b_{RX} are receiver bias, satellite bias and receiver interchannel bias respectively.
 152 $S(E)$, which is the oblique factor with zenith angle, z at IPP (Ionospheric Pierce Point) is expressed
 153 in Eq. (4).

$$154 \quad S(E) = \frac{1}{\cos(z)} = \left\{ 1 - \left(\frac{R_E \times \cos(E)}{R_E + h_S} \right)^2 \right\}^{-0.5} \quad \text{Bolaji et al. (2012)} \quad (4)$$

155 R_E = the mean radius of the earth in km and h_S = ionospheric height from the surface of the earth.
 156 According to Rama Rao et al., (2006c), ionospheric shell height of approximately 350km is
 157 appropriate for the equatorial/ low latitude region of the ionosphere for elevation cut off angle of
 158 $> 50^\circ$. This is valid in this study.

159 Hourly VTEC data obtained from these processing software are averaged to daily TEC
 160 values in TEC units ($1 \text{ TECU} = 10^{16} \text{ el/m}^2$). OBS-TEC from Birnin-kebbi, on geographic Latitude
 161 12.47° N and geographic Longitude 4.23° E located in Northern Nigeria, obtained during the

162 period 2011 – 2014, which corresponds to the ascending (2011 – 2013) and maximum (2014)
 163 phases of solar cycle 24 were compared with derived TEC obtained from International Reference
 164 Ionosphere (IRI-2016) model website
 165 (https://ccmc.gsfc.nasa.gov/modelweb/models/iri2016_vitmo.php). The 2016 version of IRI
 166 provides important changes and improvements on previous IRI versions (Bilitza et al., 2016). Solar
 167 cycle 24 is regarded as a quiet solar cycle which peaked in 2014 with maximum sunspot number
 168 (103) occurring in February. Values of sunspot number, R_z , in Text format were obtained from
 169 Space Physics Interactive Data Resource (SPIDR) website (www.ionosonde.spidr.com) shortly
 170 before it became unavailable. Table 1 shows the years used in this study and their corresponding
 171 sunspot number, R_z .

172
 173 Table I: Table of years, solar cycle phase and sunspot number, R_z [Source: Author].

Years	Solar Cycle Phase	Sunspot Number, R_z
2011	Ascending	55.7
2012	Ascending	57.6
2013	Ascending	64.7
2014	Maximum	79.6

174
 175 **2.2 METHODOLOGY**

176 Diurnal variations of hourly OBS-TEC and hourly IRI-2016 model (NeQuick topside
 177 option) were plotted using the monthly mean values of OBS-TEC and monthly mean of IRI-2016
 178 model against local time (LT) on the same Figure. The corresponding percentage deviation
 179 (percentage Dev or % DEV) of IRI-2016 from OBS-TEC were also analysed using the monthly

180 mean values of OBS-TEC and monthly mean values of IRI-2016 against local time (LT).
181 Percentage Dev is obtained using Eq. (5) below:

$$182 \quad \%DEV = \left(\frac{OBS-IRI}{OBS} \right) \times 100 \quad (5)$$

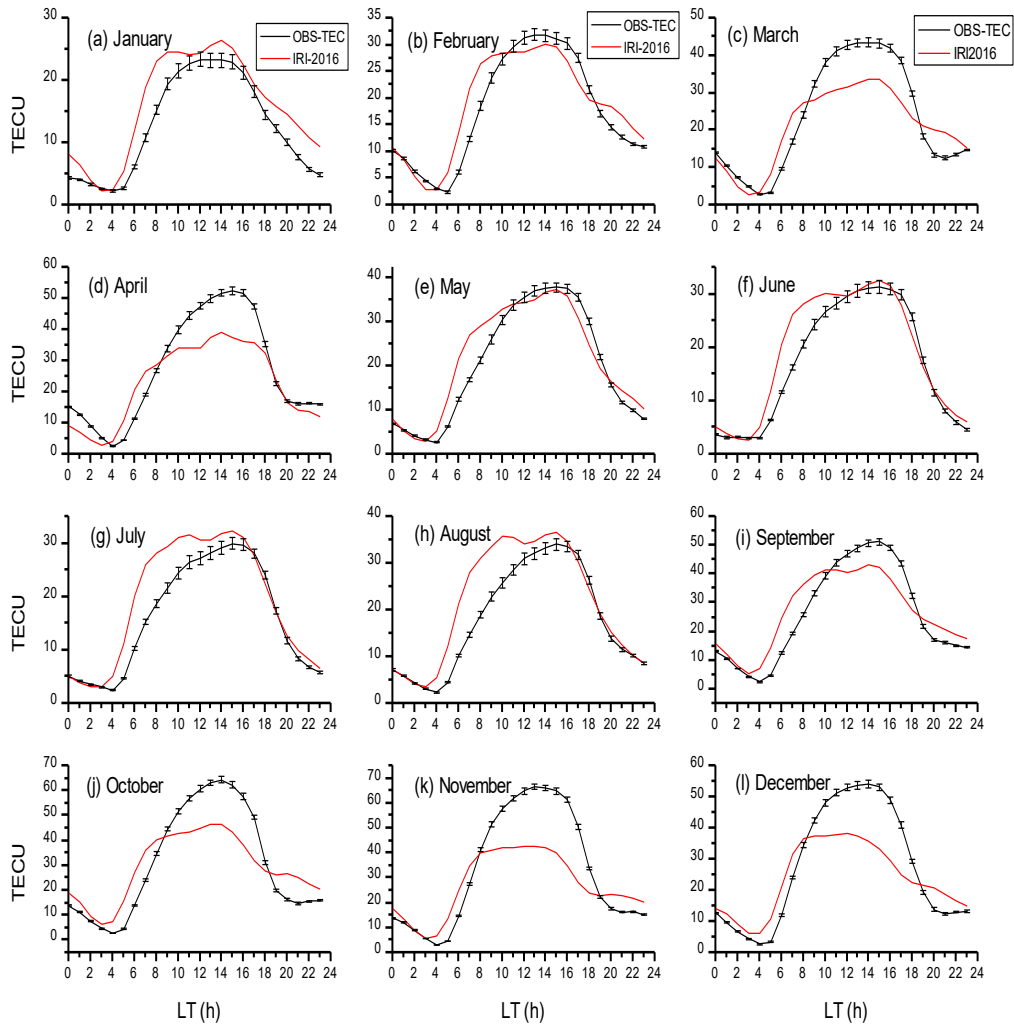
183 where OBS represents Observation-TEC values and IRI represents TEC derived by IRI-2016
184 model.

185 The OBS-TEC data was grouped following Onwumechilli and Ogbuehi (1964) into four
186 seasons namely: March equinox (February, March and April), June solstice (May, June and July),
187 September equinox (August, September and October) and December solstice (November,
188 December and January), in order to investigate seasonal variation. Finally, Annual variation of
189 OBS-TEC and sunspot number, Rz were also analysed by plotting mean OBS-TEC and mean Rz
190 against each month of the year.

191 **3 RESULT AND DISCUSSIONS**

192 Figures 1 to 4 show the diurnal variation of OBS-TEC and IRI-2016 model in the Nigerian
193 Equatorial Ionosphere (NEI) for the years 2011 to 2014 respectively. OBS-TEC were obtained
194 from the GPS receiver installed at Birnin-Kebbi station. The diurnal variation of OBS-TEC and
195 IRI-2016 model TEC reveals the typical characteristics of an equatorial/ low latitude ionosphere.
196 We show the day-to-day variation of OBS-TEC with error bar showing the standard deviation from
197 mean values. The study reveals that day-to-day variation of OBS-TEC is higher during the daytime
198 than night time for all the years. It well established known fact that during the day, the sun causes
199 variations in temperature, neutral wind, electron density and electric field thereby modulating the
200 structure and evolution of the ionosphere and thermosphere (Gorney, 1990; Forbes et al. (2006).
201 These Figs. show a steep rise in OBS-TEC from a minimum of ~2 TECU between 03:00 – 05:00
202 LT in 2011, ~3 TECU (04:00 – 05 LT) in 2012, ~3 TECU (03:00 – 05:00 LT) in 2013 and 2014.

203 OBS-TEC increased to a broad daytime maximum between 12:00 LT – 14:00 LT for all years
204 before falling to a minimum after sunset. The diurnal variation of IRI-2016 model shows TEC
205 increasing from a minimum of ~ 2 TECU in 2011, ~ 4 TECU in 2012 and 2013, and ~ 5 TECU in
206 2014 between 03:00 – 04:00 LT for all years, to a broad daytime peak between 08:00 – 14:00 LT,
207 before falling steeply to minimum before sunset. Hence the IRI-2016 model attained its peak
208 before OBS-TEC. Dabas et al. (2003); Somoye et al. (2011); Hajra et al. (2016); D’ujanga et al.
209 (2017) attributed the steep increase in TEC to the upward $\mathbf{E} \times \mathbf{B}$ vertical plasma drift and the rapid
210 filling up of the magnetic field tube at sunrise due to solar EUV ionization. During daytime, an
211 eastward electric field at the equator causes plasma to be lifted to greater heights. This dynamo-
212 generated eastward electric field combined with the northward geomagnetic field lifts the
213 equatorial ionosphere from 700 km to 1000 km, resulting in additional ionization (D’ujanga et al.,
214 2017; Somoye et al., 2011). Suranya et al., 2015 further mentioned that upward vertical $\mathbf{E} \times \mathbf{B}$ drift
215 could lead to equatorial ionization anomaly (EIA) and meridional winds. The magnetic field tubes
216 then collapse after sunset due to low thermospheric temperature and Rayleigh Taylor Instability
217 (RTI) (Berkner and Wells, 1934) giving rise to the minimum TEC values after sunset. These results
218 are similar to findings of Bolaji et al., (2012), Fayose et al., (2012), Okoh et al., (2014), Eyelade
219 et al., (2017) who have explored the NEI.



220 Fig. 1: Diurnal variation of OBS-TEC showing error bar and IRI-2016 model of each month during
 221 January – December 2011 at Birnin-Kebbi

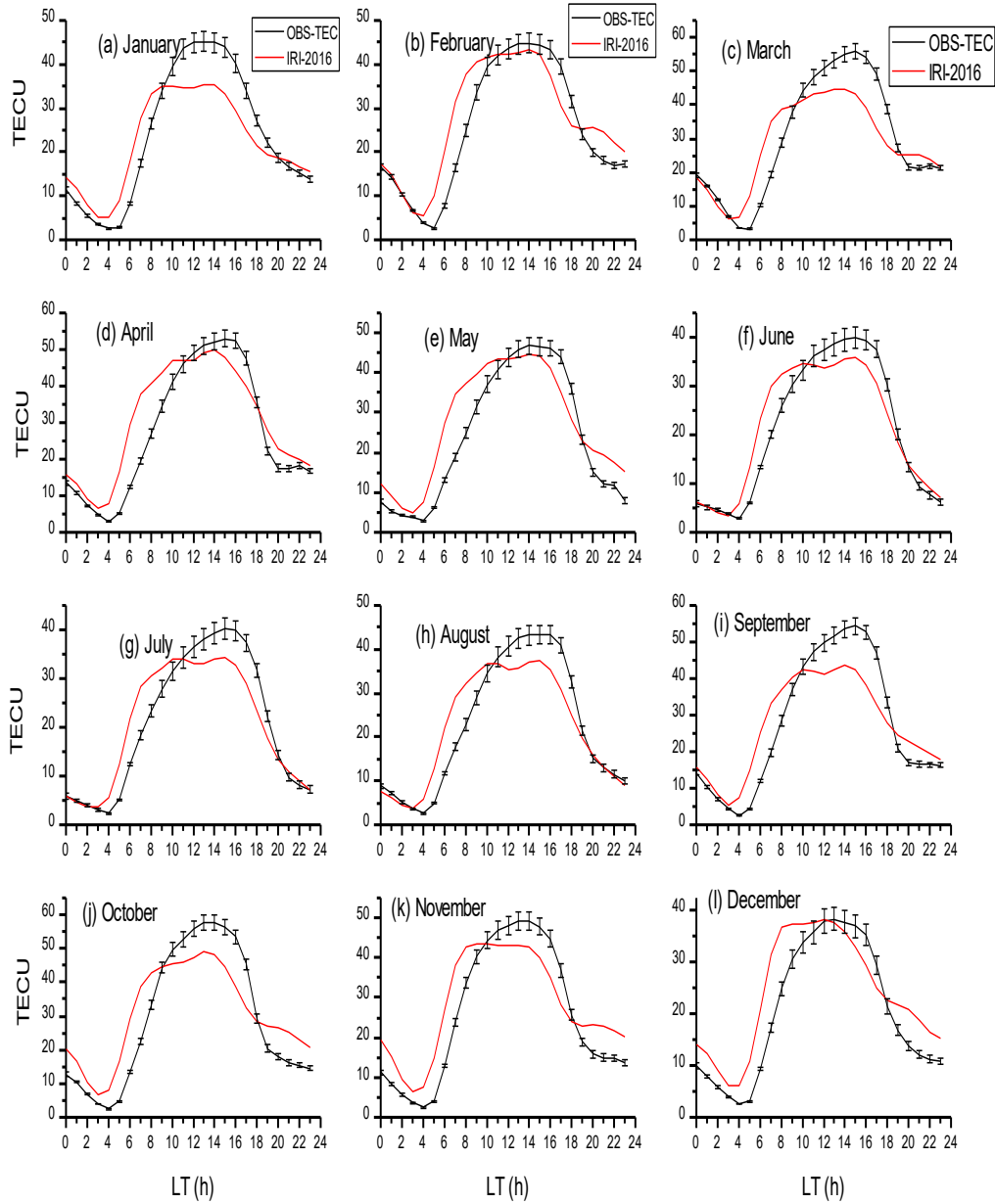


Fig. 2: Same as Figure 1 for 2012.

222

223

224

225

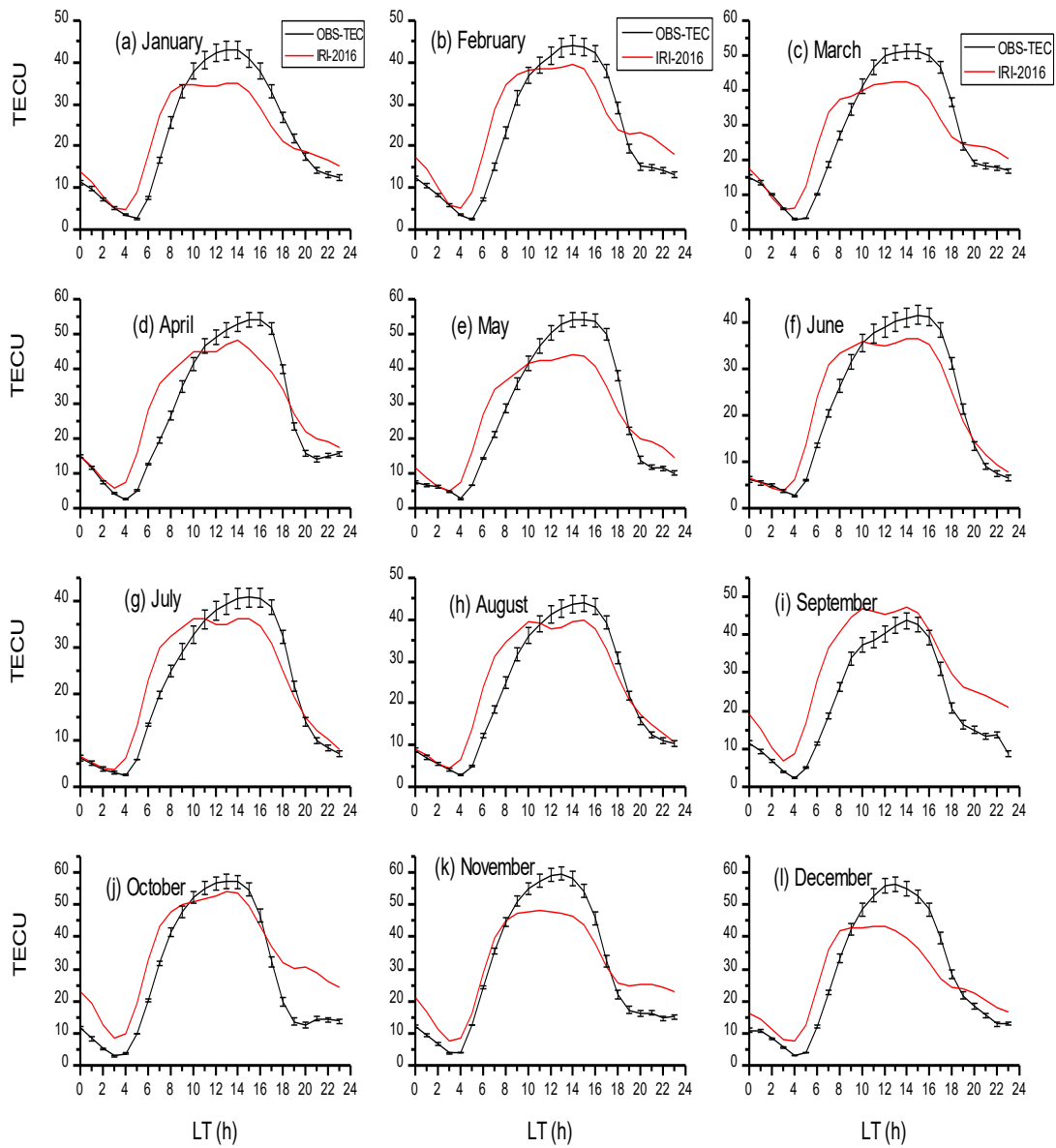


Fig. 3: Same as Figure 1 for 2013.

226

227

228

229

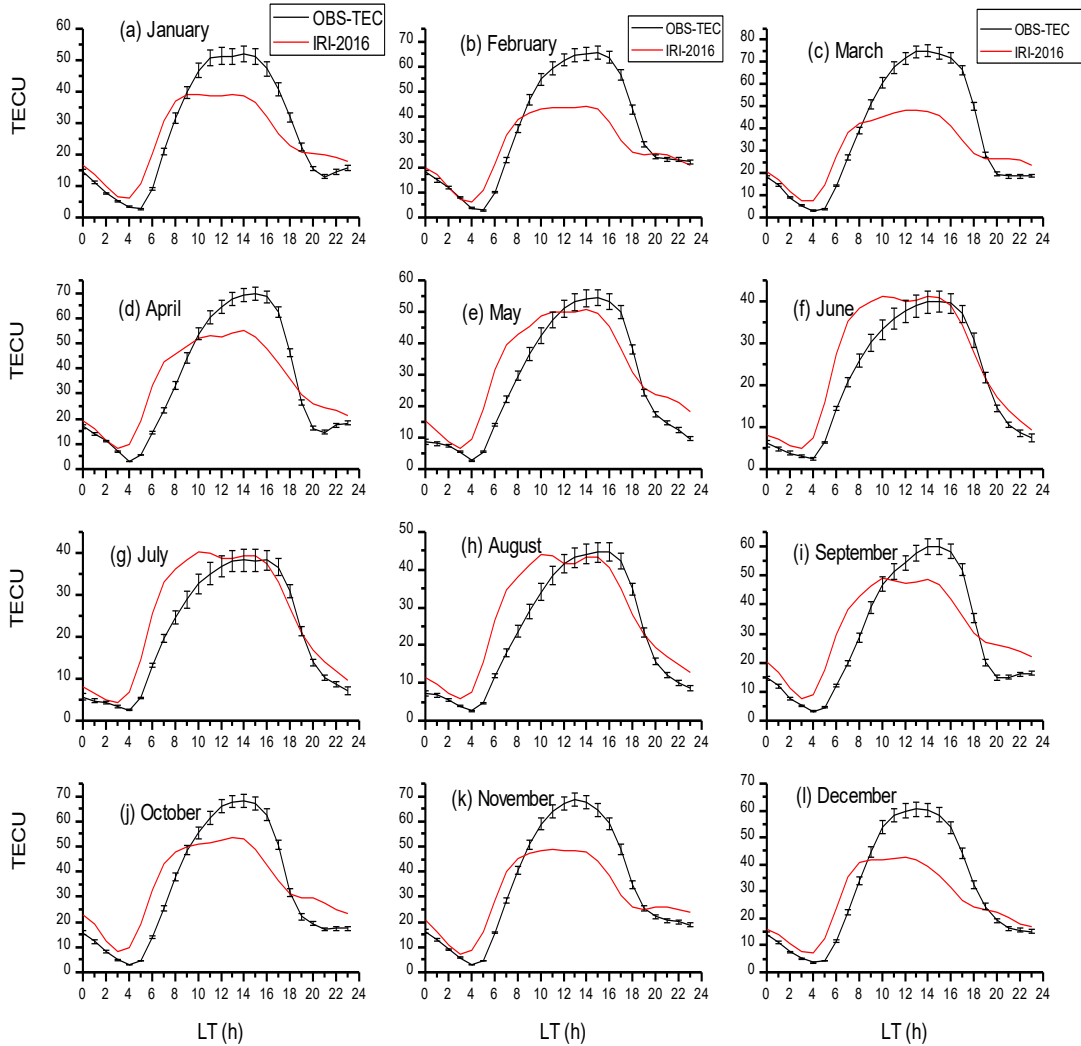


Fig. 4: Same as Figure 1 for 2014.

230

231

232

233

234

235

236

It can be seen that OBS-TEC is much higher in 2014 with maximum value up to 70 TECU in March compared with IRI-2016 maximum of 54 TECU in the month of October, 2014. The diurnal variation reveals that the peak of OBS-TEC of majority of the months for all years shifted to slightly post-noon hours (13:00 – 14:00 LT). This type of peak shifting is peculiar to equatorial/ low latitude regions and the Polar Regions of the ionosphere and it is found to depend on the equatorial ionization anomaly and solar zenith angle respectively (Rama Rao et al., 2009; D’ujanga

237 et al., 2017). Another key observation seen in the diurnal variation of OBS-TEC is the post-sunset
238 decrease and slight enhancement in some months. The night time enhancement of TEC, for
239 example, March, April and October of the year 2011, March and April of the year 2012, March,
240 April, September and October of the year 2013, January, April and September of the year 2014
241 was documented by previous researchers like Rama Rao et al., 2009; D’ujanga et al., 2017 and
242 Ayorinde et al., 2016. They attributed it to the product of eastward and westward directed electric
243 field which produces an upward and downward motion of ionospheric plasma during the day and
244 night respectively.

245 Figures 5 to 8 show the diurnal variation of percentage deviation of IRI-2016 model from
246 OBS-TEC in the Nigerian Equatorial Ionosphere (NEI) for all years respectively. On a general
247 note, IRI-2016 model only presented suitable predictions for the post-midnight hour between 00 –
248 03 LT of the day for all years. All other hours from 04 – 23 LT show some discrepancies. In fact,
249 for some of the months: October, November and December of 2012, October and December, 2013,
250 and September and October of 2014, these discrepancies lasted throughout the day. Whereas in
251 some other months: June, July and August of 2011, June, July and August of 2012, June and
252 August of 2013 and February, June and July of 2014, these discrepancies collapsed during the pre-
253 midnight hours (18 – 23 h). It is also important to mention that IRI-2016 model either over
254 estimated or under estimated TEC in the NEI especially during daytime hours as shown in the
255 plots.

256

257

258

259

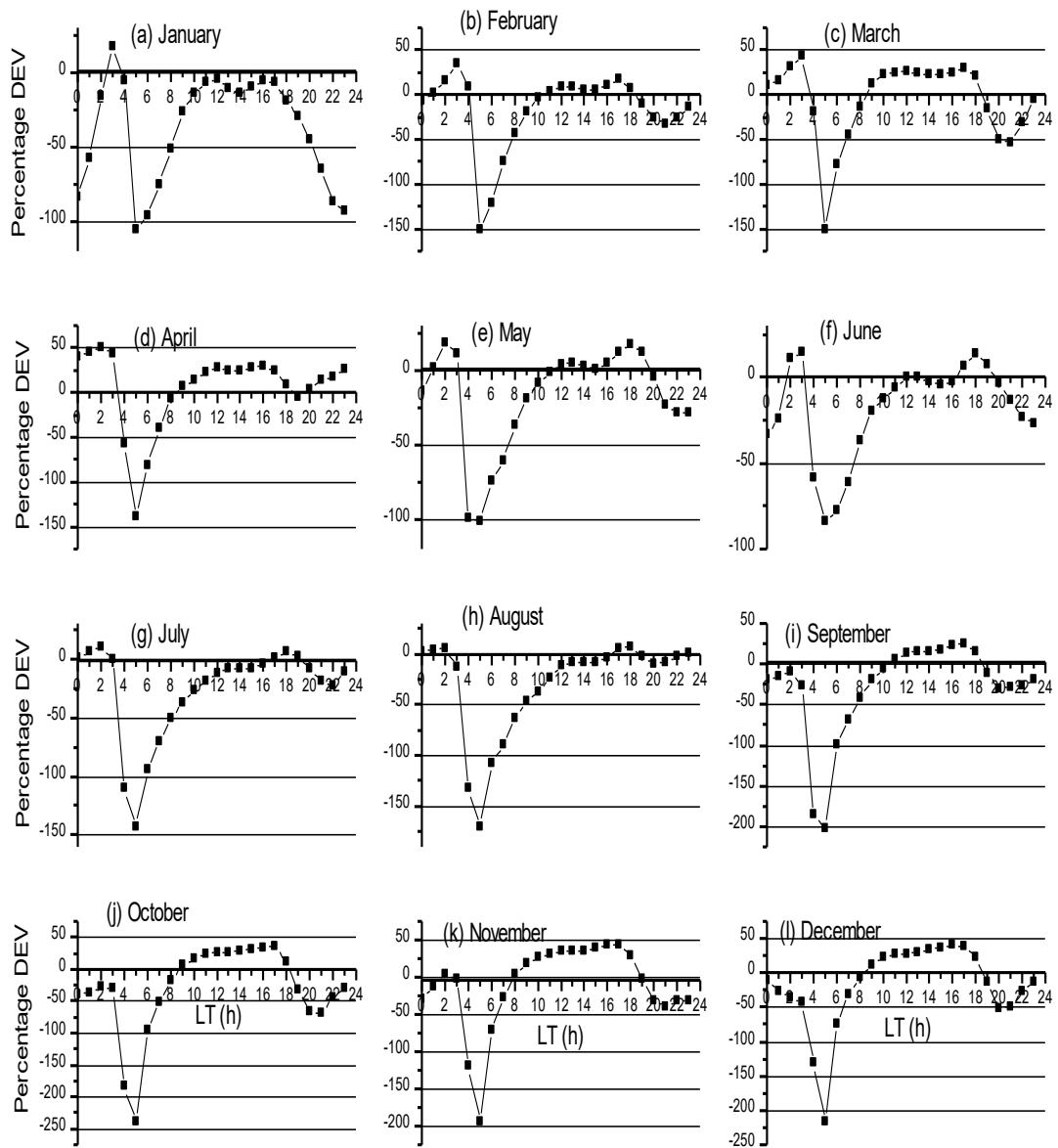


Fig. 5: Percentage deviation of IRI-2016 from OBS-TEC for year 2011

260

261

262

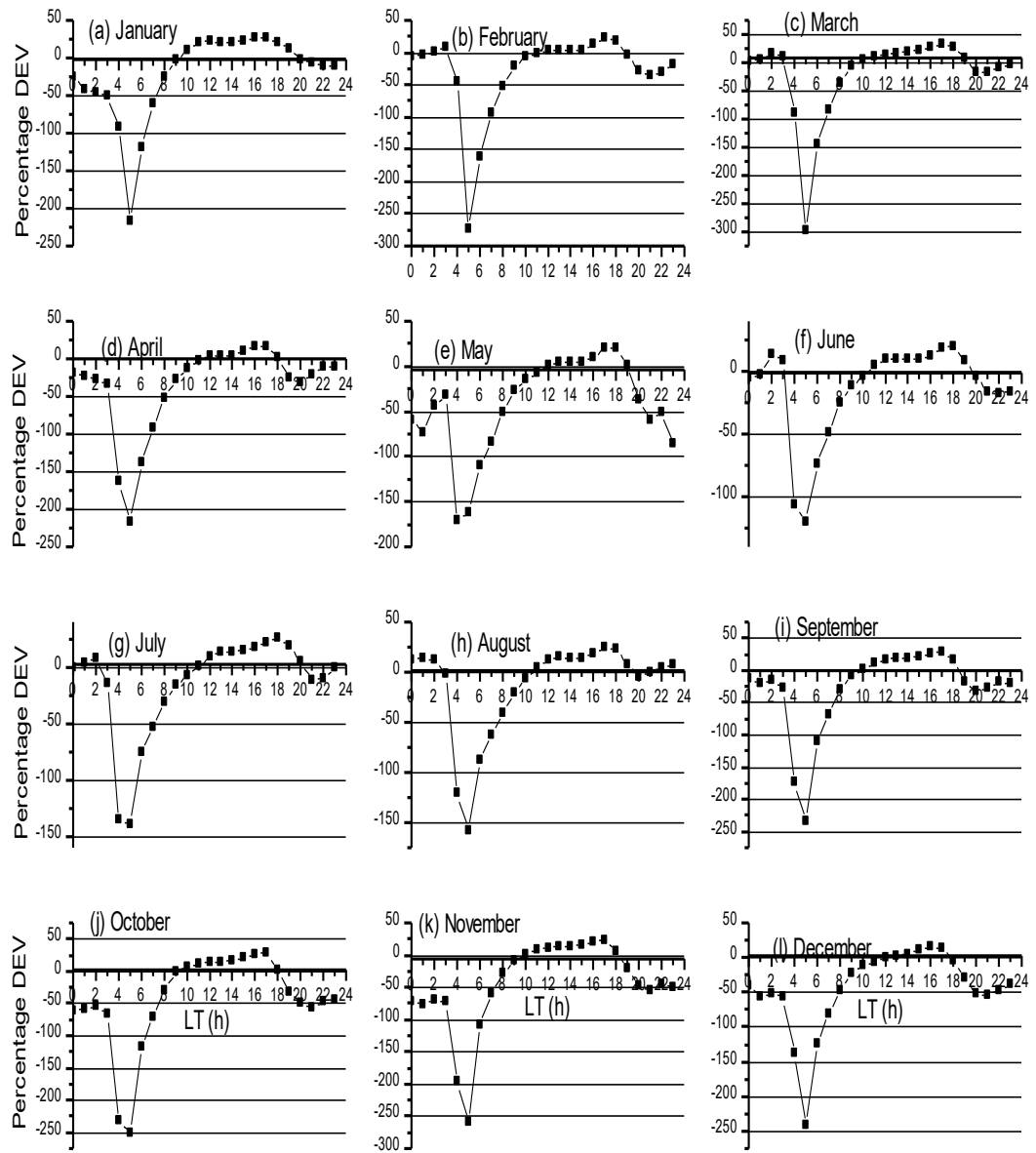


Fig. 6: Percentage deviation of IRI-2016 from OBS-TEC for year 2012

263

264

265

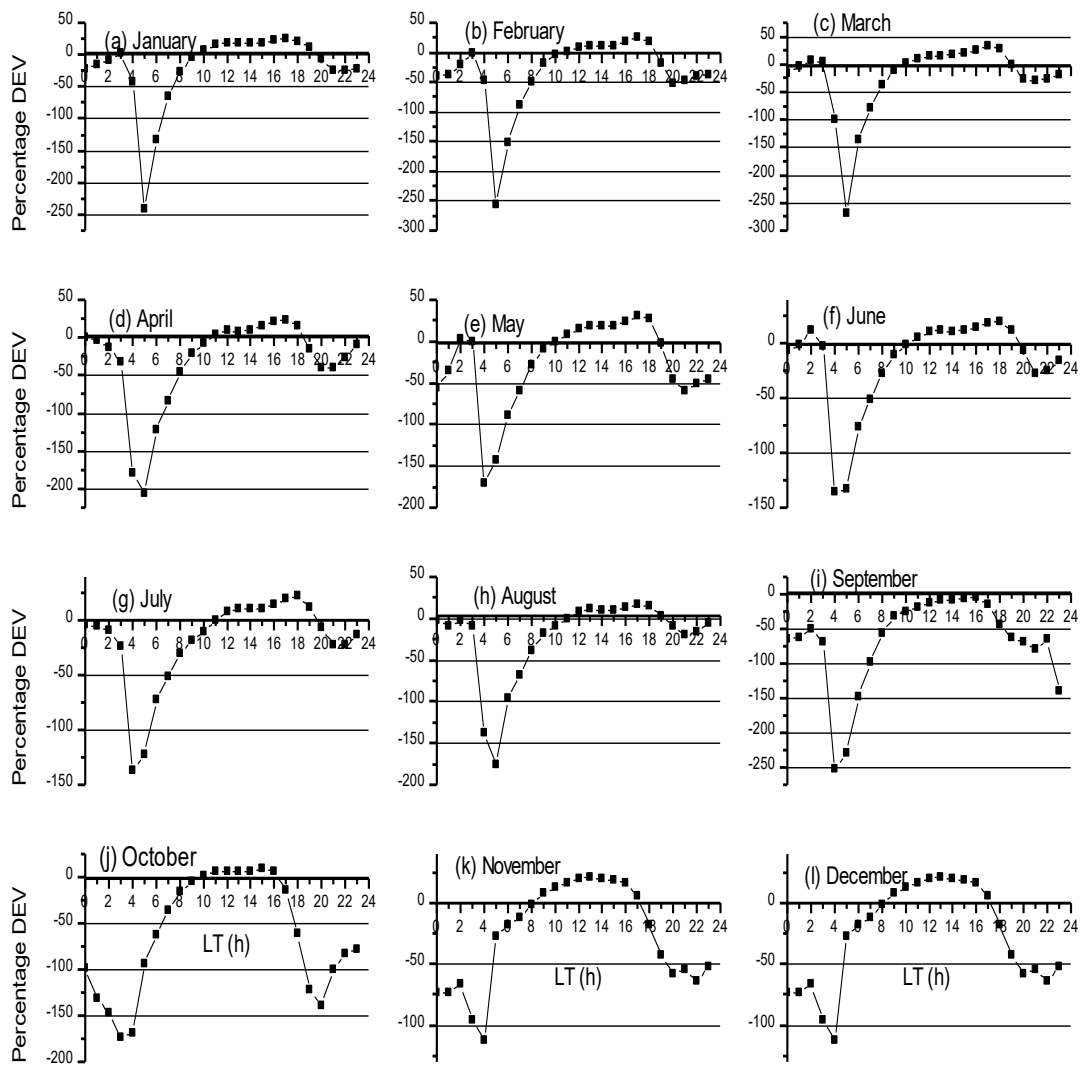


Fig. 7: Percentage deviation of IRI-2016 from OBS-TEC for year 2013

266

267

268

269

270

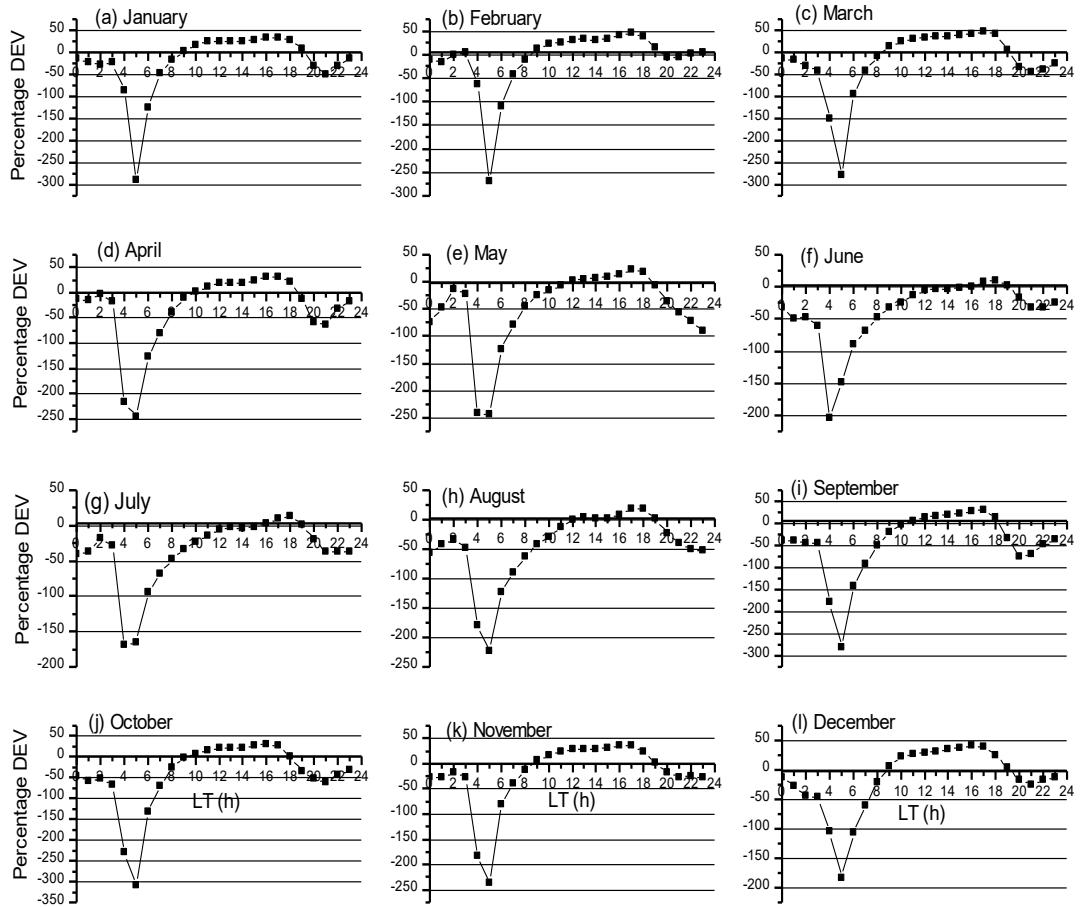


Fig. 8: Percentage deviation of IRI-2016 from OBS-TEC for year 2014

271

272 The mass plots in Fig. 5 – 8 further reveal that negative percentage deviation shows higher
 273 values of IRI-2016 than OBS-TEC values. The reverse is the case for positive percentage
 274 deviation. Highest negative percentage deviations are seen between 04 – 05 LT for all months
 275 throughout the years in this study. Highest Negative percentage deviation of ~ 300% was recorded
 276 in the month of October, 2014 at 05 LT. Table II shows the summary of months with daytime
 277 over- or under-estimate of IRI-2016 in the NEI.

278

279

Table II: Months of daytime estimate of IRI-2016 model in NEI [Source: Author]

YEAR	OVER ESTIMATE	UNDER ESTIMATE	SAME RANGE
2011	January, July, August	February – April, September - December	May - June
2012		January - December	
2013	September	January – August, October - December	
2014		January - December	

280

281 Therefore, it is clear from Fig. 1- 4, Fig. 5 – 8 and Table II that IRI-2016 model did not
 282 predict well in the NEI. This may be attributed to insufficient data which is as a result of the sparse
 283 distribution of GPS infrastructure in this region. Our result agree with those Komjathy et al. (1998);
 284 Lee and Reinisch (2006); Malik et al. (2016). Bhuyan and Borah (2007) reported higher IRI TEC
 285 than their measured values at about all local time in their location. Mosert et al. (2007) and Sethi
 286 et al. (2010) also reported discrepancies between of IRI TEC predictions and GPS TEC during
 287 high solar activity (HSA) and low solar activity (LSA) respectively at equatorial/ low latitudes.

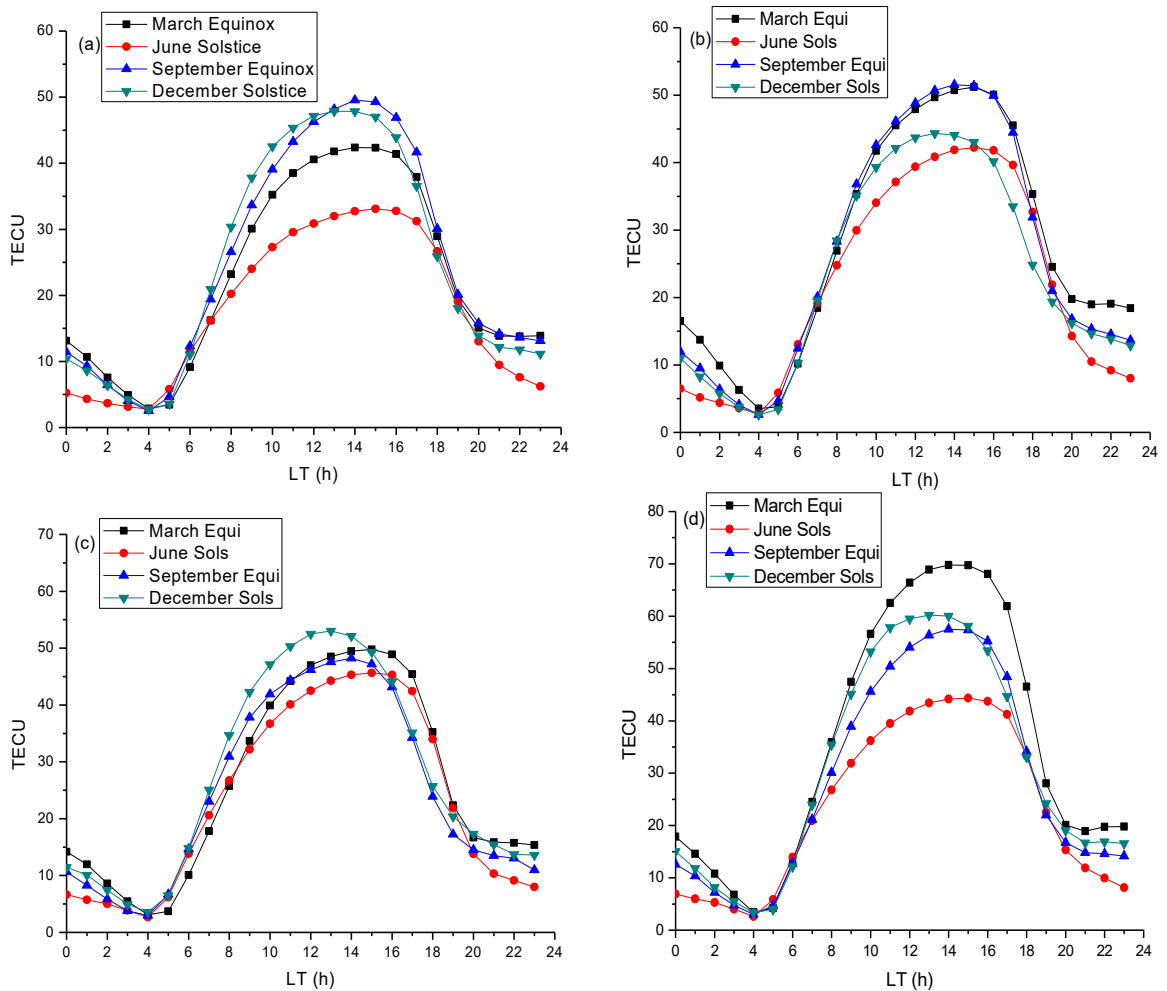
288 Figure 9 show the seasonal variations of OBS-TEC for the four years investigated. The
 289 change in concentration of Oxygen and molecular Nitrogen has been reported to be the main cause
 290 of seasonal variation of ionospheric parameters. Seasonal variation of OBS-TEC in this study
 291 depicts semi-annual variation with equinoctial maximum (~ 52 TECU) and solsticial minimum (~
 292 44 TECU) in 2012. D’ujanga et al., (2017) reported that since the sun passes through the equator
 293 during the equinox, both March and September equinox experience the same solar radiation. It is
 294 also a well-established fact that March 20 and September 23 are the only times in the year when

295 the solar terminator is perpendicular to the equator, giving rise to the equinoctial maximum. The
296 semi-annual variation resulting from the effect of equatorial ionization anomaly (EIA) in the
297 ionosphere has been attributed to the effect of solar zenith angle and magnetic field geometry (Wu
298 et al., 2008; Rama Rao et al., 2006a). Another important feature of ionospheric parameters (known
299 as equinoctial asymmetry) which is reported in the work of Bolaji et al., (2012); Akala et al.,
300 (2013); Eyelade et al., (2017); D'ujanga et al., (2017); Aggarwal et al., (2017), is clearly seen in
301 all years used in this work. Akala et al., (2013) also reported minimum and maximum seasonal
302 VTEC values during June solstice and December solstice respectively, during ascending phase of
303 solar cycle 24. Equinoctial asymmetry is a strong phenomenon that occurs at low latitudes
304 (Aggarwal et al., 2017), which has been explained in terms of the differences in the meridional
305 winds leading to changes in the neutral gas composition during the equinoxes.

306

307

308



309 Fig. 9: Seasonal variation of observed OBS-TEC during (a) 2011 (b) 2012 (c) 2013 and (d)
 310 2014

311 In 2011, September equinox and December solstice recorded higher magnitude, followed
 312 by March equinox; the lowest was in June solstice. In 2013, December solstice magnitude was
 313 highest, followed by the equinoxes, March and September respectively and lowest in June solstice.
 314 This corresponds to result obtained by Akala et al. (2013), which they attributed to increase in ion
 315 production rate in winter season and anti-correlation between December and June Solstice pre-
 316 reversal velocity enhancement. In 2014, March equinox magnitude was highest, December solstice
 317 and September equinox magnitudes were about same range while June solstice magnitudes were

318 least. December solstice magnitude is found to occur between the magnitudes of the equinoxes in
319 2011 and 2014. The September equinox magnitude and March equinox magnitude are observed to
320 interchange in 2011 and 2014. Overall, June solstice magnitudes were lowest during all the years.
321 Titheridge (1974) attributed the June solstice least magnitudes to low ionization resulting from
322 reduced production rates, i.e. O/ N₂ ratio.

323 Also, for all seasons, pre-midnight (18 – 23 LT) values of TEC are higher than post-
324 midnight (00 – 05 LT) TEC values for all years. In 2011, pre- midnight TEC values are in the
325 range of 8 – 30 TECU while post-midnight TEC values ranges from 3 to 13 TECU. In 2012, pre-
326 midnight TEC values are in the range of 9 – 35 TECU while post-midnight TEC values are between
327 3 to 17 TECU. In 2013, the pre-midnight TEC values are between 9 – 35 TECU while post-
328 midnight TEC values ranges from 3 – 15 TECU. Finally in 2014, pre-midnight TEC values are
329 between 9 to 47 TECU while the post-midnight TEC ranges from 3 to 18 TECU. Furthermore, the
330 maximum OBS-TEC values in 2011 (49 TECU) and 2012 (52 TECU) were recorded in September
331 Equinox season. In 2013, OBS-TEC reached a maximum of 53 TECU in December solstice while
332 in 2014, the maximum OBS-TEC (70 TECU) was recorded in March Equinox season in the NEI
333 (West African sector). This result agrees in general with those of D’ujanga et al. (2017) who
334 obtained higher TEC values during the equinoxes than during the solstices in Ethiopia (East
335 African sector). This same result was observed by Bagiya et al. (2009) that reported higher TEC
336 values in equinoctial months than solstitial months in the Indian sector. While the former authors
337 reported maximum TEC of ~ 58 TECU during the equinox months, the latter authors reported
338 maximum TEC ~ 50 TECU during the equinoxes. Seasonal variation of TEC is dependent on
339 thermospheric neutral compositions since during the day the equator is hotter than the pole.
340 Meridional winds therefore flows from the equator towards the pole. This flow cause a change in

341 the neutral composition resulting in the decrease of the ratio of O/ N₂ at the equator. The decrease
 342 of O/ N₂ ratio increases the electron density, and thus resulting in TEC increase during the
 343 equinoxes (Bagiya et al., 2009). The corresponding annual range error (meters) of the season with
 344 maximum OBS-TEC using 1 TECU variation to represent an error of 0.16 m in position is
 345 summarized in Tables III.

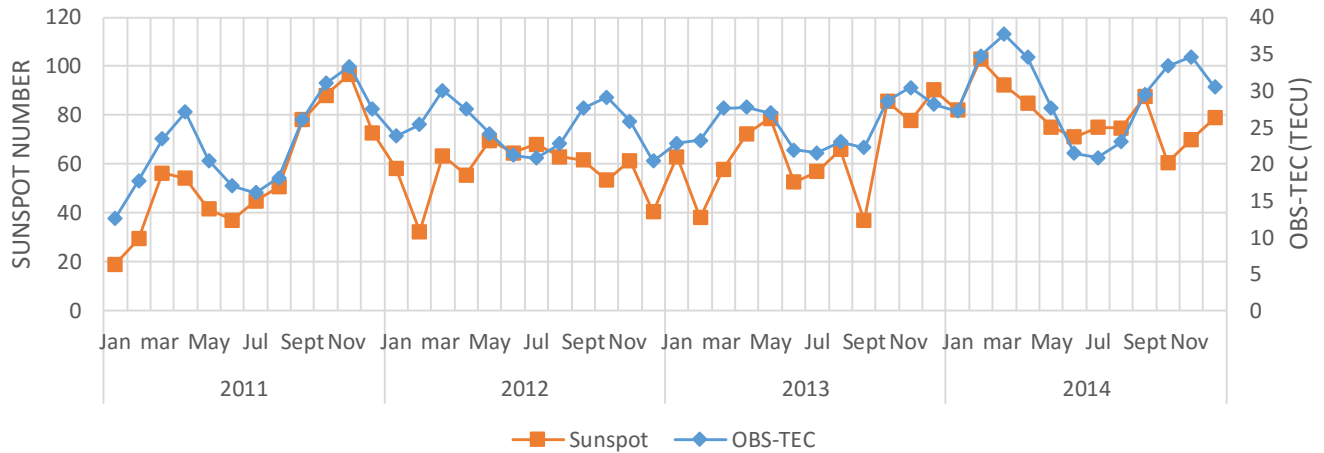
346 Table III: Season of maximum OBS-TEC and their corresponding range error.

YEAR	SEASON OF MAXIMUM OBS-TEC	VALUE (TECU)	CORRESPONDING ERROR (m)
2011	September Equinox	49	8
2012	September Equinox	52	8
2013	December Solstice	53	8
2014	March Equinox	70	11

347

348 Figure 10 shows the comparison of the monthly mean OBS-TEC and monthly mean
 349 sunspot number, R_z from 2011 – 2014, showing an increase and decrease of TEC following the
 350 solar cycle variations. Our result is in good agreement with those of Chakrabarty et al. (2012) and
 351 D’ujanga et al. (2017), which reported a direct solar cycle effect on TEC measurements. Solar
 352 cycle dependency of ionospheric parameters such as TEC provides useful information to study the
 353 behavior and variations of the physical and photochemical processes in the ionosphere (Liu et al.
 354 2006). It is well documented that the variability of solar activity results in huge variations in the
 355 temperature, neutral wind, neutral density, ion and electron densities and electric fields in the
 356 ionosphere (Forbes et al. 2006).

357



358

Figure 10: Monthly variation of OBS-TEC with sunspot number, Rz at Birnin-Kebbi

359

360 The present result also agrees with that of Rama Rao et al. (1985) who reported a direct
 361 solar control on TEC. Balan et al. (1994); Liu et al. (2011) and Liu et al. (2006) and many other
 362 works reported the same results during low and moderate solar activity, TEC and N_mF_2 increases
 363 linearly with solar proxies, but the linearity collapse during high solar activity. This agrees with
 364 our result except for July month of 2012 and 2014 which shows saturation effect on TEC i.e
 365 decrease in TEC with increase in solar activity. The saturation effect on TEC was reported in the
 366 work of Balan et al. (1994, 1996), which concluded that the saturation effect has not been clarified
 367 and hence might be due to other factors near the earth's environment and not as a result of the
 368 influence of solar activity. We could not establish the cause of the saturation effect on TEC in this
 369 study, however, saturation effect will be further investigated in future studies.

370 **4 CONCLUSIONS**

371 Studies on OBS-TEC and IRI-2016 model at Birnin-Kebbi in Northern Nigeria during the
 372 ascending and maximum phases of solar cycle 24 have been carried out. Our result shows that
 373 OBS-TEC and IRI-2016 model rising from a minimum in the early hours of the day to a broad

374 daytime maximum before falling steeply to a minimum after sunset for all years, due to
375 photoionization increase produced by solar extreme ultraviolet (EUV) radiation (Anderson et al.,
376 2004; D’ujanga et al., 2017). The diurnal variation reveals that the peak of OBS-TEC is often
377 delayed when compared with IRI-2016 model, with the maximum occurring afternoon, showing
378 dome-like shape while noon bite-out, a special feature observed in equatorial/ low latitude is seen
379 in the peak of majority of the plots of IRI-2016 model. On a general note, we concluded that IRI-
380 2016 model cannot be used as proxy for TEC measurements for most hours of the day for the years
381 investigated. Our result agree with those of Komjathy et al. (1998); Lee and Reinisch (2006); Malik
382 et al. (2016); Bhuyan and Borah (2007); Mosert et al. (2007) and Sethi et al. (2010) at their
383 respective locations. For all seasons, pre-midnight (18 – 23 h) values of TEC are higher than post-
384 midnight (00 – 05 h) TEC values during all years. Seasonal variation shows an asymmetry in the
385 equinoxes and solstices in the NEI as also reported by Fayose et al. (2012) and Eyalade et al.
386 (2017). Maximum OBS-TEC values in 2011 and 2012 were recorded in September equinox. In
387 2013, OBS-TEC reached its maximum during the December solstice while in 2014, the maximum
388 OBS-TEC was recorded in March equinox. This result agrees in general with those of D’ujanga et
389 al. (2017) in the East African sector and Bagiya et al. (2009) in the Indian sector, who obtained
390 higher TEC values during the equinoxes than during the solstices. Thermospheric neutral
391 compositions is a major cause of seasonal variation of ionospheric parameters such as TEC, since
392 during the day the equator is hotter than the poles. Finally, monthly OBS-TEC varies linearly with
393 annual sunspot number, R_z , thus revealing strong dependence of TEC on solar activity (sunspot
394 number). This linearity collapsed in the month of July of 2012 and 2014. OBS-TEC and sunspot
395 number were found to increase gradually from 2011 to 2014 in agreement with Rama Rao et al.
396 (1985) showing that there is a direct solar control on TEC.

397 **ACKNOWLEDGEMENT**

398 We thank the Office of the Surveyor General of the Federation (OSGoF-Nigeria) for making TEC
399 data available through the infrastructure www.nignet.net. We also thank Hatanaka, Y., Gopi
400 Krishna for providing TEC processing software online. Finally, we appreciate Bilitza et al. (2017)
401 for making the latest version of IRI model available online.

402 **REFERENCES**

403 Aggarwal, M., Bardhan, A., Sharma, D.K. Equinoctial asymmetry in ionosphere over Indian
404 region during 2006 – 2013 using COSMIC measurements. *Advances in Space Res.*, 60, 999 –
405 1014, 2017.

406 Akala, A.O., Somoye, E.O, Adeloye, A.B., Rabiou, A.B. Ionospheric f_oF_2 variability at equatorial
407 and low latitudes during high, moderate and low solar activity. *Indian Journal of Radio and Space*
408 *Physics*. Vol. 40, 124 – 129, 2011.

409 Akala, A.O., Seemala, G.K., Doherty, P.H., Valladares, C.E., Carrano, C.S., Espinoza, J., and
410 Oluyo, K.S. Comparison of equatorial GPS-TEC observations over an African station and an
411 American station during the minimum and ascending phases of solar cycle 24. *Ann. Geophys.*, 31,
412 2085, 2013.

413 Alizadeh, M.M., Wijaya, D.D., Hobiger, T., Weber, R., Schuh, H. Ionospheric effects on
414 microwave signals in J. Bohm and H. Schuh (eds). *Atmospheric Effect in Space Geodesy*. Springer
415 atmospheric sciences. Doi: 10.1007/978-3-642-36932-2_2, © Springer-Verlag Berlin Heidelberg,
416 2013.

417 Anderson, D., Anghel, A., Chau, J., Veliz, O. Daytime vertical $\mathbf{E} \times \mathbf{B}$ drift velocities inferred from
418 ground-based magnetometer observations at low latitudes, *Space Weather*, 2, S11001; doi:
419 10.1029/2004SW000095, 2004.

420 Ayorinde, T.T., Rabiou, A.B., and Amory-Mazaudier, C. Inter-hourly variability of Total Electron
421 Content during the quiet condition over Nigeria within the Equatorial Ionization Anomaly region.
422 *J. Atmos. Solar Terr. Phys.*, 145, 21 – 33, 2016.

423 Berkner, L.V. and Wells, H.W. F-region ionosphere – investigation at low latitude. *Terres. Magn.*,
424 39, 215, 1934.

425 Bagiya, M.S., Joshi, H.P., Iyer, K.N., Aggarwal, M., Ravin-dran, S., and Pathan, B.M. TEC
426 variations during low solar activity period (2005 – 2007) near the Equatorial Ionization Anomaly
427 Crest region in India. *Ann Geophys.*, 27, 1047 – 1057, 2009.

428 Balan, N., Bailey, G.J., Moffett, R.J. Modelling studies of ionospheric variations during an intense
429 solar cycle. *J. Geophys. Res.*, 99, 17467 – 17475, 1994.

430 Balan, N., Bailey, G.J., Su, Y.Z. variations of the ionosphere and related solar fluxes during solar
431 cycle 21 and 22. *Advances in Space Res.*, 18, 11 – 14, 1996

432 Bhuyan, P.K. and Borah, R.R. TEC derived from GPS network in India and comparison with the
433 IRI. *Advances in Space Res.*, 39, 830 – 840, 2007.

434 Bilitza, D., Altadill, D., Zhang, Y., Mertens, C., Truhlik, V., Richards, P., McKinnell, L.A.,
435 Reinisch, B. International reference ionosphere 2012 – A model of international collaboration. *J.*
436 *Space Weather Space Clim.*, 4, 1 – 12, doi: 10.1002/201JA018009, 2014.

437 Bilitza, D., Altadill, D., Truhlik, V., Shubin, V., Galkin, I., Reinisch, B., and Huang, X.
438 International reference ionosphere 2016: from ionospheric climate to real-time weather
439 predictions. *Space weather*, 15, 418 – 429, doi: 10.1002/20165SW001593, 2016.

440 Bolaji, O. S., Adeniyi, J.O., Radicella, S.M., and Doherty, P.H. Variability of total electron content
441 over an equatorial West African station during low solar activity. *Radio Sci.*, 47, RS1001, doi:
442 10.1029/2011RS004812, 2012.

443 Chakrabarty, D., Bagiya, M.S., Thampi, S.V., Iyer, K.N. Solar EUV flux (0.1 – 50 nm), $F_{10.7}$ cm
444 flux, sunspot number and total electron content in the crest region of the ionization anomaly during
445 the deep minimum between solar cycle 23 and 24. *Indian Radio and Space Phys.*, 41, 110 – 120,
446 2012.

447 Ciraolo, L., and Spalla, P. TEC analysis of IRI simulated data. *Adv. Space Res.*, 29, 6, 959 – 966,
448 2002.

449 Codrescu, M. V., Palo, S. E., Zhang, X., Fuller-Rowell, T. J., Poppe, C. TEC climatology derived
450 from TOPEX/POSEIDON measurements, *Journal of Atmospheric Solution*, 61, 281-298, 1999.

451 Dabas, R.S., Singh, L., Lakshmi, D.R., Subramanyam, P., Chopra, P., Garg, S.C. Evolution and
452 dynamics of equatorial plasma bubbles: relationships to $\mathbf{E} \times \mathbf{B}$ drifts, post-sunset total electron
453 content enhancements, and equatorial electrojet strength. *Radio Sci.*, 38, doi:
454 10.1029/2001RS002586, 2003.

455 D’ujanga, F.M., Opio, P. Twinomugisha, F. Variation of total electron content with solar activity
456 during the ascending phase of solar cycle 24 observed at Makerere University, Kampala. *Space*
457 *Weather: Longitude and Hemispheric Dependences and Lower Atmosphere Forcing*, Geophysical
458 Monograph 220, First Edition. Edited by Timothy Fuller-Rowell, Endawoke Yizengaw, Patricia

459 H. Doherty, and Sunanda Basu. © 2017 American Geophysical Union. Published 2017 by John
460 Wiley & Sons, Inc., 2017.

461 Eyelade, V.A., Adewale, A.O., Akala, A.O., Bolaji, O.S. and Rabiou, A.B. Studying the variability
462 in the diurnal and seasonal variations in GPS TEC over Nigeria. *Ann. Geophys.*, 35, 701 – 710,
463 2017.

464 Fayose, R.S., Rabiou, B., Oladosu, O., Groves, K. Variation of total electron content (TEC) and
465 their effect on GNSS over Akure. Nigeria, *Applied Physics Research*, 4, 2, 2012.

466 Forbes, J.M., Bruinsma, S., Lemoine, F.G. Solar rotation effects in the thermospheres of Mars
467 and Earth. *Science*, 312, 1366–1368, 2006.

468 Gorney, D. J. Solar cycle effects on the near-earth space environment. *Rev Geophys*, 28, 315–
469 336, 1990.

470 Hajra, R., Chakraborty, S.K., Tsurutani, B.T., DasGupta, A., Echer, E., Brum, C.G.M., Gonzalez,
471 W.D., Sobral, H.A. An empirical model of ionospheric total electron content (TEC) near the crest
472 of the equatorial ionization anomaly (EIA). *J. Space Weather Space Clim.*, 6, A29, doi:
473 10.1051/swsc/2016023, 2016.

474 Jee, G., Schunk, R. W., Scherliess, L. Analysis of TEC data from the TOPEX/Poseidon mission,
475 *Journal of Geophysical Research*, 109, A01301, doi:10.1029/2003JA010058, 2004.

476 Komjathy, A., Langley, R., Bilitza, D. ingesting GPS-derived data into the IRI for single frequency
477 radar altimeter ionospheric delay corrections. *Adv. Space Res.*, 22, 6, 793 – 802, 1998.

478 Langley, R., Fedrizzi, M., Paula, E., Santos, M., Komjathy, A. Mapping the low latitude
479 ionosphere with GPS. *GPS World*, 13, 2, 41 – 46, 2002.

480 Lee, C.C. and Reinisch, B.W. Quiet condition hmF2, NmF2 and Bo variations at Jicamarca and
481 comparison with IRI-2001 during solar maximum. *J. Atmos. Solar Terr. Phys.*, 68, 2138 – 2146,
482 2006.

483 Liu, L., Wang, W., Chen, Y., Le, H. Solar activity effects on the ionosphere: A brief review. *Space*
484 *Physics and Space Weather Geophysics. Chinese science Bulletin.* 56, 12, 1202 – 1211, 2011.

485 Liu, L., Wang, W., Ning, B., Pirog, O.M., and Kurkin, V.I. Solar activity variations of the
486 ionospheric peak electron density. *J. Geophys. Res.*, vol 111, A08304, doi:
487 10.1029/2006JA011598, 2006

488 Malik, R.A., Abdullah, M., Abdullah, S., Homam, M.J. Comparison of Maximum Useable
489 Frequency (MUF) variability over Peninsular Malaysian with IRI Model during the rise of solar
490 cycle 24. *J. Atmos. Solar Terr. Phys.*, 138 – 139, 87 – 92, 2016.

491 Maruyama, T., Ma, G., and Nakamura, M. Signature of TEC storm on 6 November 2001 derived
492 from dense GPS receiver network and ionosonde chain over Japan. *Journal of Geophysical*
493 *Research*, 109, A10302, doi: 10.1029/2004JA010451, 2004.

494 Mosert, M., Gende, M., Brunini, C., Ezquer, R. and Altadill, D. Comparisons of IRI TEC with
495 GPS and Digisonde measurements at Ebro. *Advances in Space Res.*, 39, 841 – 847, 2007.

496 Okoh, D., Lee-Anne McKinnell, L., Cilliers, P., Okere, B., Okonkwo, C., Rabiou, A.B. IRI-VTEC
497 versus GPS-vTEC for Nigerian SCINDA GPS stations. *Advances in Space Research*,
498 <http://dx.doi.org/10.1016/j.asr.2014.06.037>, 2014.

499 Ogunmodimu, O., Rogers, N.C., Falayi, E., Bolaji, S. Solar Flare induced cosmic noise absorption,
500 *NRIAG Journal of Astronomy and Geophysics.* 7, 1, 31-39, 2018.

501 Ogwala, A., Somoye, E.O., Oyedokun, O., Adeniji-Adele, R.A., Onori, E.O., Ogungbe, A.S.,
502 Ogabi, C.O., Adejo, O., Oluyo, K.S., Sode, A.T. Analyses of Total Electron Content over Northern
503 and Southern Nigeria. *J. Res. and Review in Sci.*, 21 – 27, 2018.

504 Onwumechilli, C.A., and Ogbuehi, P.O. *Journal Atmos. Terr. Phys.*, 26, 894, 1964.

505 Rama Rao, P.V.S., Niranjana, K., Rama Rao, B.V., Rama Rao, B.V.P.S., Prasad, D.S.V.V.D. Proc.
506 URSI/ IPS Conference on the ionosphere and Radio wave Propagation. Sydney, Australia, 1985.

507 Rama Rao, P.V.S., Krishna, S.G., Prasad, J.V., Prasad, S.N.V.S., Prasad, D.S.V.V.D., Niranjana,
508 K. Geomagnetic storm effects on GPS based navigation. *Ann. Geophys.*, 27, 2101 – 2110, 2009.

509 Rama Rao, P.V.S., Krishna, S.G., Niranjana, K., Prasad, D.S.V.V.D. Study of temporal and spatial
510 characteristics of L-band scintillation over the Indian low-latitude region and their possible effects
511 on GPS navigation. *Ann. Geophys.*, 24, 1567 – 1580, 2006a.

512 Rama Rao, P.V.S., Krishna, S.G., Niranjana, K., Prasad, D.S.V.V.D. Temporal and spatial
513 variations in TEC using simultaneous measurements from Indian GPS network of receivers during
514 low solar activity period of 2004 – 2005. *Ann. Geophys.*, 24, 3279 – 3292, 2006b.

515 Rama Rao, P.V.S., Niranjana, K., Prasad, D.S.V.V.D., Krishna, S.G., Uma, G. On the validity of
516 the ionospheric pierce point (IPP) altitude of 350km in the Indian equatorial and low-latitude
517 sector. *Ann. Geophys.*, 24, 2159 – 2168, 2006c.

518 Sethi, N. K., Pandey, V. K., Mahajan, K. K. Comparative study of TEC with IRI model for solar
519 minimum period at low latitude. *Advances in Space Research*, 27, 45 – 48, 2010.

520 Suranya, P.L., Prasad, D.S.V.V.D., Niranjan, K., Rama Rao, P.S.V. Short term variability in foF2
521 and TEC over low latitude stations in the Indian sector. *Indian J. of Radio and Space Phys.*, 44, 14
522 – 27, 2015.

523 Somoye, E.O. Diurnal and seasonal variation of fading rates of E- and F-region echoes during IGY
524 and IQSY at the equatorial station of Ibadan. *Indian Journal of Radio and space Physics*, 38, 194
525 – 202, 2010.

526 Somoye, E.O., Akala, A.O., Ogwala, A. Day-to-day variability of h'F and foF2 during some solar
527 cycle epochs. *Journal Atmos. Solar Terr. Physics*, 73, 1915 – 1922, 2011.

528 Stankov, S. M. Trans-ionospheric GPS signal delay gradients observed over mid-latitude Europe.
529 *Advances in Space Research*, 43, 1314–1324, 2009.

530 Sunda, S. and Vyas, B.M. Local time, seasonal and solar cycle dependency of longitudinal
531 variations of TEC along the crest of EIA over India. *J. Geophys. Res.*, vol 118, 6777 – 6785, 2013.

532 Tariku, Y.A. Pattern of GPS-TEC variability over low-latitude regions (African sector) during the
533 deep solar minimum (2008 to 2009) and solar maximum (2012 to 2013) phases. *Earth, Planets,*
534 *and space*. 67, 35, 2015.

535 Titheridge, J.E. Changes in atmospheric composition inferred from ionospheric production rates.
536 *J. Atmos. Terr. Phys.*, 36, 1249 – 1257, 1974.

537 Torr, M.R. and Torr, D.G. The seasonal behavior of the F2 layer of the ionosphere. *J. Atmos. Terr.*
538 *Phys.*, 35, 2237, 1973.

539 Tsai Ho-Fang, Liu Jann-Yenq, Tsai Wei-Hsiung and Liu Chao-Han, Tseng Ching-Liang and Wu
540 Chin-Chun. Seasonal variations of the ionospheric TEC in Asian equatorial anomaly regions. *J.*
541 *Geophysical Res.*, vol 106, A12, 30,363 – 369, 2001.

- 542 Wanninger, L. Effects of the equatorial ionosphere on GPS. *GPS World*, 2, 48, 1993.
- 543 Wu, C.C., Liou, K., Shan, S.J., Tseng, C.L. Variation of ionospheric total electron content in
544 Taiwan region of the equatorial anomaly from 1994 – 2003. *Adv. Space Res.*, 41, 611 – 616, 2008.
- 545